INCREASING THE SPATIAL ACCURACY OF THE LAND USE MAP USING FUSION OF OPTICAL AND RADAR IMAGES OF SENTINEL AND GOOGLE EARTH ENGINE

J. Jafarzadeh [1]*, S. Attarchi [2]

[1] PhD candidate, Geography Faculty, University of Tehran, Tehran, I.R. Iran – jafar.jafarzadeh@ut.ac.ir
[2] Geography Faculty, University of Tehran, Tehran, I.R. Iran – satarchi @ut.ac.ir

Commission IV, WG IV/3

KEY WORDS: land use, sentinel, radar, optics, decision tree, engine inheritance.

ABSTRACT:

Nowadays, exact and real-time land use and land cover (LULC) maps are imperative to supply precise data for energetic observing, arranging and arrive administration. With the appearance of cloud computing frameworks, time arrangement includes extraction methods, and machine learning classifiers, unused openings emerge in more precise and larger-scale LULC mapping. In this research, the aim is to obtain a land use map with a spatial resolution of 10 meters by combining Sentinel-1 radar images and Sentinel-2 optical images. The processing was done in Google Earth Engine cloud computing system. Also, in this research, NDVI map and NDBI map were used to increase classification accuracy. Classification was done using the decision tree method and in eleven classes. To evaluate the classification accuracy and the final map, randomly collected points were used in the study area. The results of the comparison of the ground collection points and the final classified map showed that the classification accuracy in this study was around 94%. The results obtained from such as research can be optimally used in urban planning and crisis management.

1. INTRODUCTION

1.1 Theoretical Foundations

In studies related to cities, it is important to know the distribution and dispersion of urban land as well as its different uses, because the land located within the limits of a city has a significant impact on the microclimate of the region, the amount of energy consumed and the provision of services in the city by service sectors (Seto et al., 2011). Arnold and Gibbon (1996) consider urban land to be synonymous with impervious land, that is, areas of the city such as roads, residential areas, industrial sectors and other areas that are made of materials impermeable to water such as asphalt, concrete and stone, and the sizes are different; For example, these levels can include a small private house to the largest commercial or entertainment centres. When it rains, these impervious areas flow a large volume of water on their surface and no water infiltration takes place in them .As a result, they increase flood flows. Even built-up urban lands play a significant role in absorbing solar energy and forming urban heat islands; Therefore, by examining and comparing these lands in different years, the direction and method of physical expansion of cities can be studied (Mohammadnejad Arouq, 2019).
Exact and real-time land use and land cover (LULC) maps are imperative to supply exact data for energetic arrive checking, arranging and administration. With the appearance of cloud computing stages, time arrangement highlights extraction methods, and machine learning classifiers, modern openings emerge in more precise and larger-scale LULC mapping (Nasiri et al., 2022). Arrive utilize maps are essential information sources for arrive arranging and administration (Esfandeh et al., 2021; Yao et al., 2022). Precise and up-to-date arrive use/land cover (LULC) mapping has continuously been of intrigued to the geographical and inaccessible detecting communities (Qian and Zhang, 2022; Schulz et al, 2021; Viana et al., 2019). Mainly because it provides valuable information for understanding human-environment relationships (Praticò et al., 2019; Sobhani, et al., 2021).
Built-up urban lands are synonymous with impervious urban surfaces. These parts are very important for managers and urban planners; Because the study of the location and dispersion of built-up areas, the density of these areas and the process of its changes over time has been important, and city managers must have sufficient and up-to-date knowledge of these changes for better management; Therefore, they can plan the current development process of the city and its future changes based on sustainable development (Attarchi, 2018). Considering that the physical development of the city is a dynamic and continuous process during which the physical limits of the city increase in vertical and horizontal directions, qualitatively and quantitatively, access to information and data of these changes is usually done using land mapping, which is a costly and expensive task. It is time-consuming and it is not possible to repeat it for consecutive years; Therefore, it is possible to study and examine the physical changes of cities by using remote sensing techniques and processing different satellite images, at high speed and as a time series. Usually, these images are an important source for studying land cover and their changes in cities.
On the other hand, these images can provide data about urban heat islands, the urban environment and its changes, and ultimately modelling the city's development. The available sensors operate in different parts of the electromagnetic spectrum, which mainly include the optical, thermal and radar parts. The first sensors were active in the optical and thermal sector; Therefore, they have good historical data. Also, their access and analysis are relatively simple, but at the same time,

* Corresponding author

https://doi.org/10.5194/isprs-annals-X-4-W1-2022-321-2023

they also have disadvantages; For example, we can mention the possibility of similarity of spectral response of different complications in these images. Also, if the area is covered with clouds, optical images will not be able to record the image of the earth's surface. On the other hand, thermal data usually have little spatial resolution and are associated with great limitations in studies related to cities. Meanwhile, radar sensors operate in the microwave range of the electromagnetic spectrum, but compared to optical images, they are more complicated and difficult to analyse. Therefore, if different images from different sources can be integrated and used in urban studies, more accurate results will be obtained (Gomez et al., 2006).

Finally, combining radar and optical images is a suitable method for urban studies (Hass and Ban, 2017; Pavanelli et al., 2018). The Google Earth Engine (GEE) framework may be a web-based and cloud computing framework created by Google for the reason of putting away and dissecting a tremendous sum of information on a petabyte scale (counting different toady pictures, advanced rise models, climate information, vector information) has been propelled (Seto et al., 2011). A very good feature of this system is that it is free, does not require advanced and expensive hardware, and has free and online access to the European and American Space Agency databases and many other databases (Shelestov et al., 2017; Goldblatt, 2016; Patel., 2015). In this research, the aim is to extract a land use map with high spatial accuracy by combining the optical and radar images of the Sentinel satellite. This work was done in the environment of the Google Earth Engine system with the regression method, and as a result, it led to the extraction of a ten-meter land use map with eleven different classes and with the decision tree classification method. By using the collected points on the ground and matching them with the obtained map, the accuracy of 94% of this classification was confirmed. The innovation of this research is the use of the linear regression method to combine radar and optical images and extract a ten-meter land use map with high accuracy.

1.2 Materials and Methods

1.2.1 Study area

Ardabil area has a zone of 17,800 square kilometers within the northwest of Iran's level. This area is found between the topographical arranges of 37.45 to 39.42 and the north scope of 48.55 to 47.3 within the east of the Greenwich Meridian. Ardabil city is one of the cities of Iran and the middle of Ardebil territory within the north-west of the nation. The range of this city is 3810 km2, and the common confront of Ardebil city is influenced by tall elevation of the Savalan Mountains (Sabalan), Baghru (Talesh) and Bazgosh, and all these normal variables have caused it to be encased.

Ardabil is an ancient city in north-western Iran, and the capital of Ardabil Province. As of the 2022 census, Ardabil's population was 588,000. The dominant majority in the city are ethnic Iranian Azerbaijanis and the primary language of the people is Azerbaijani. Ardabil is known for its trade in silk and carpets. Figure 1 shows the location of the study area.

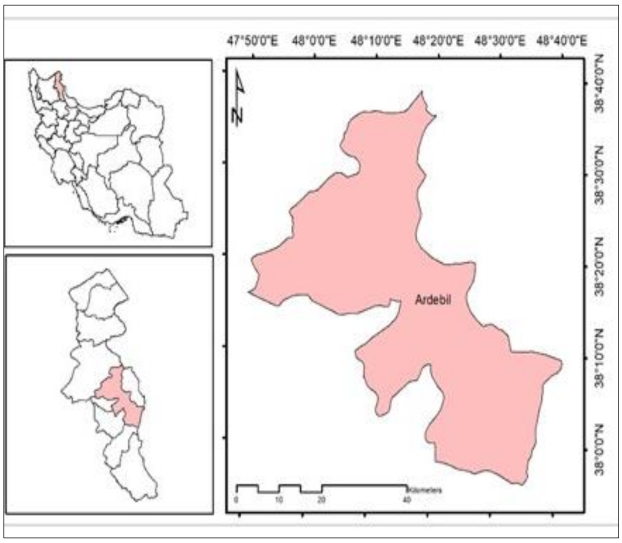

Figure 1. The study area.

1.2.2 Data used

Table 1 shows the data used in this research. ArcGIS software version 8.10 and satellite image processing software ENVI version 5.3 are used in this research.

Data	Purpose	Source	Spatial resolution	Temporal resolution	Sensor
S-1C	Classification and fusion	Copernicus Open Access Hub	10 m	6 days	SAR
S-2A	Classification and fusion	Copernicus Open Access Hub	10 m, 20 m, 60 m	5 days	MSI
Global land cover maps	Quantitative validation	Copernicus Land Service	100 m	1 year	Proba-V

Table 1. Sources and reason of the datasets utilized within the think about with details (Shrestha et al., 2021).

1.3 Research Methods

Figure 2 illustrate the research process. The steps of pre-processing, processing and post-processing of these images include several different steps that are implemented in different software. First, we pre-process and process the images of Sentinel One and Two satellites using the special Sentinel image processing software, that is, SNAP software. Then we calculate the indicators introduced in the article by using ENVI software. Then we apply the calculated indices on the sentinel images. Finally, using the Google Earth Engine environment, we combine the images to get the final image. We prepare the final integrated image in the ArcGIS software environment to prepare the final map and cartography.

https://doi.org/10.5194/isprs-annals-X-4-W1-2022-321-2023 |

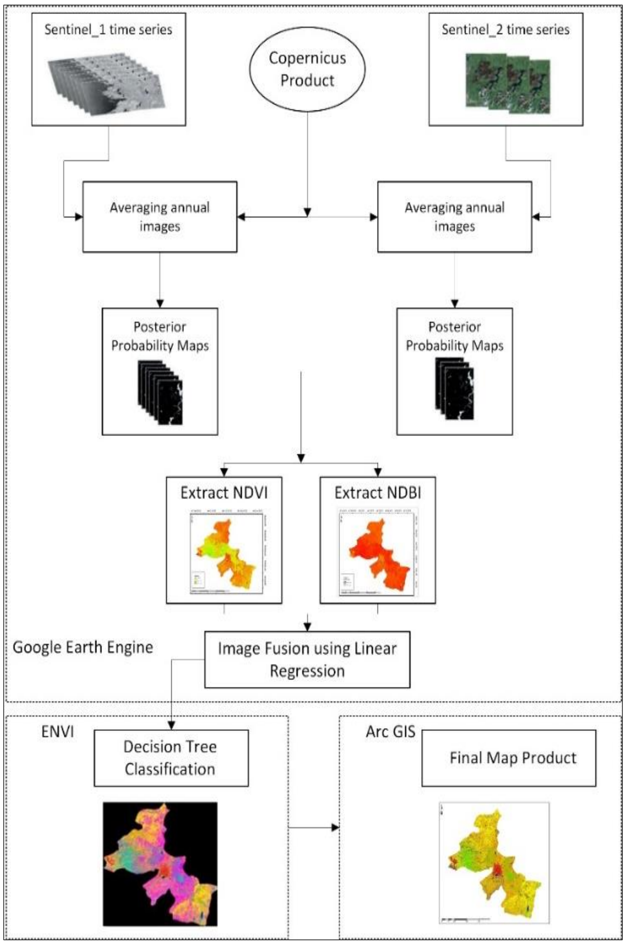

Figure 2. Research process.

1.3.1 Normalized Differential Vegetation Index (NDVI)

The Normalized Difference Vegetation Index (NDVI) may be a straightforward graphical file that's utilized in inaccessible detecting examination and estimations to survey the nearness or nonappearance of vegetation in an region. The range of changes of this index is between +1 and -1. This index is calculated through equation 1 (Gates, 1980):

$$NDVI = \frac{(NIR-RED)}{(NIR+RED} \tag{1}$$

Where NIR=Near Infra-Red Band
RED= Red Band

1.3.2 Simple Linear Regression

If only one independent variable is used to identify and predict the dependent variable, the model is called simple linear regression. The form of the linear regression model from equation 2 is as follows:

$$Y = \beta_0 + \beta_1 x + \epsilon \tag{2}$$

As you can see, this relationship is the equation of a line to which the error term or ϵ has been added. The parameters of this linear model are the width from the origin (β0) and the slope of the line (β1). The slope of the line in simple linear regression shows how sensitive the dependent variable is to the independent variable. It means that by increasing one unit to the value of the independent variable, how much the dependent variable will change. The width from the origin also represents the value of the dependent variable, which is calculated for the value of the independent variable equal to zero. In another way, the constant value or width from the origin can be considered as the average value of the dependent variable in exchange for removing the independent variable (Rasoulinia and Sharifi, 2021).

1.3.3 Normalized Difference Built-up Index (NDBI)

Image classification procedure (supervised classification and unsupervised classification) is long and complex prepare. It requires compositive band & apply numbers of operation for the ultimate result. The exactness determined from picture classification method depends on the picture investigator & strategy taken after by examiner. Be that as it may, NDBI calculation is basic and simple to determined. NDBI can be calculated by taking after equation.

$$NDBI = \frac{(\text{SWIR} - \text{NIR})}{(\text{SWIR} + \text{NIR})} \tag{3}$$

For Landsat 7 data,
NDBI = (Band 5 – Band 4) / (Band 5 + Band 4),
for Landsat 8 data, NDBI = (Band 6 – Band 5) / (Band 6 + Band 5)
and for Sentinel-2 data, Default rendering is Normalized Difference Built-Up Index computed as SWIR(Band11)-NIR(Band8)/ SWIR(Band11) +NIR(Band8).
Moreover, the Normalize Distinction Build-up Record esteem lies between -1 to +1. Negative esteem of NDBI speak to water bodies though higher esteem speaks to build-up regions. NDBI esteem for vegetation is moo (Chunyang et al., 2010). samples are judged. This means that we randomly select samples from two different communities, regardless of whether the number of samples is equal or unequal, and compare the averages of those two communities. (Mansour Far, 2014).

2. RESULTS AND DISCUSSION

After collecting the required data, in the Google Earth Engine environment, the method of integration of sentinel radar and optical images was coded. First, the shape file of the studied area was called in the Google Earth Engine system. In order to facilitate classification, it is first necessary to enter a 100-meter land use map product into the system as a guide. Then we call Sentinel 1 radar images for the desired date and region in the system, which are in VV and VH polarization. The reason for choosing these two types of polarization is that there are usually plenty of images of these two types of polarization to obtain land use maps, and other polarizations are rarely available for this purpose.
After that, we enter Sentinel 2 images into the system. Then the Sentinel 1 data, we average the images for one year and then cut the obtained images for the desired area. Next, we convert the radar image from decibel to backscattering. The decibel(dB) image values are usually between negative one and zero, but the backscattering image values are between zero and one, which results in creating a strong contrast for the image. In the next step, we enter the Sentinel 2 image into the system by applying a time filter and a location filter for the desired region and the desired date. Then, using a cloud display filter, we select and import relevant images with less than ten percent clouds. In the next step, like the Sentinel 1 image, using a median filter, we select the images that have less than ten percent cloud cover and the highest

reflectivity. Sentinel 2 bands used for this research are bands 2, 3, 4 and band 8. In the next step, we will produce normalized differential vegetation index map and normalized differential construction index. These indicators can be calculated using bands 2 to 4 and 8 of Sentinel 2. Figure 3 and Figure 4 show the normalized differential vegetation index and the normalized differential construction index, respectively.

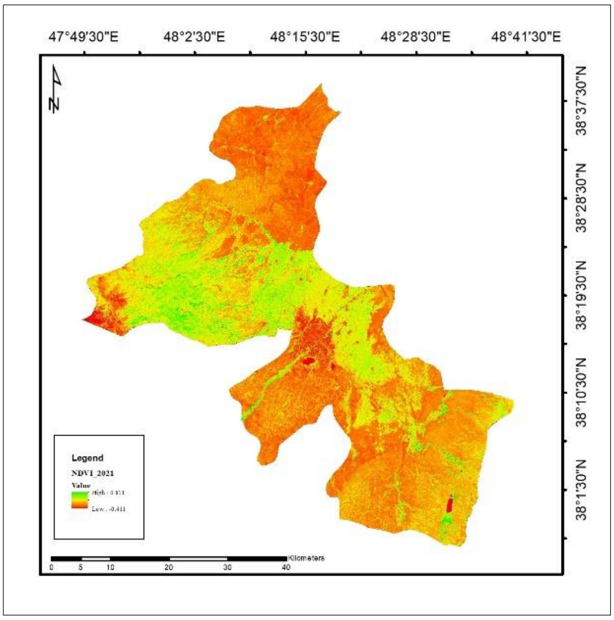

Figure 3. Normalized differential vegetation cover index for the study area for 2021.

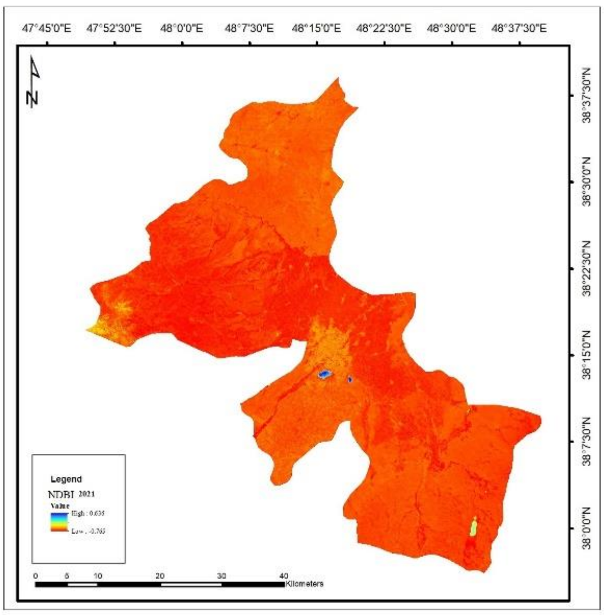

Figure 4. Normalized Difference Built-up index for the study area for 2021.

Next, we create a dataset of radar and optical data. To this dataset, let's add the data related to the hundredth product. This is because we will take classification samples from this product. We determine the amount of sample that is necessary to collect for classification. The sample taken should be less than 5000 samples. We must determine the amount of the sample so that our method does not suffer from errors. In this research, since the goal is to determine eleven different classes and classes, we will consider one hundred samples for each class and finally we will have 1200 samples, which is a good distance from the quorum of 5000 samples. Sample collection is done automatically in this method. We consider the result obtained from this section as training data. The primary classification method for combining two data in this research is random forest method. Finally, after preliminary calculations and preliminary classification based on the centennial product of land use, we extract the final map and enter it into Envi's image processing software environment by outputting it. In this software, using the decision tree classification method, we reclassify the final map obtained from the Google Earth Engine system. We consider eleven different classes according to the Copernicus standard and according to the definitions provided for each class. The number of classes may be different for different regions. To make sure how many classes are there in the study area, the number of twenty classes can be considered first, and after classification by decision tree method, it can be seen that some classes are missing in the study area and finally the number The final classes of this area can be seen. Figure 5 illustrated the final ten-meter land use map for the study area in eleven different classes.

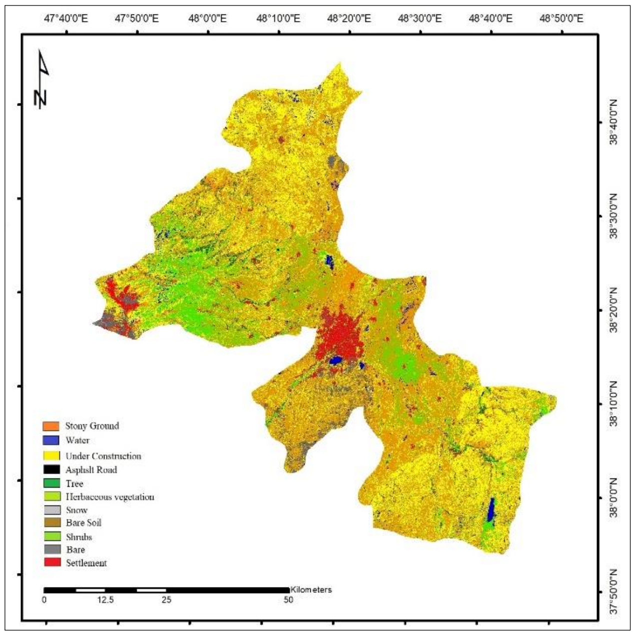

Figure 5. The final land use map.

To evaluate the accuracy of the classification, after collecting fifty ground points with a single-frequency hand-held GPS device, the classified classes were matched with the ground control points, and the results indicate that the accuracy of the classified data is 94%.

3. CONCLUSION

Access to a proper map of earth effects and phenomena is very important, because these effects and the process governing them are the source of many risks and environmental resources. The utilize of fitting strategies and up-to-date adj. pictures in different thinks about, particularly urban considers, can have a awesome effect on the generation of urban maps. One of these imperative information is the outline related to the limits of urban lands, which can be extricated utilizing distinctive strategies. This research created a land use map with a spatial resolution of 10 meters using the integration of Sentinel satellite radar and optical images using the simple linear regression method and the classification method using the decision tree method. The number of training points collected in this research, which was done automatically and through the Google Earth Engine system, was 1200 samples. The number of ground control points to evaluate the accuracy of the classification was 50 points, which by matching with the final map, it was determined that the accuracy of this method was 94%. The results of this research show that the combination of SAR time series images of Sentinel 1 and Sentinel 2 and their use in the semi-automatic extraction of urban lands can overcome many of the limitations of image classification methods on a regional scale, such as analysing one by one images of different regions, time limitations in Collecting a large number of ground control points eliminates the need for complex algorithms and downloading a large amount of data. Also, the results show that the use of radar data can be widely used, especially in the study and extraction of built-up urban lands (impenetrable lands) because they have the ability to record images in any weather conditions and at any hour of the day and night. Because the reflection of radar waves is very strong in urban areas. Another important result of this article is the identification of the very high efficiency of the GEE system in processing a huge amount of satellite images. The use of this system does not require any specialized remote sensing software, and the user can easily process various data using a computer browser or even his phone. Another vital point is that in this framework there's no got to download diverse images, but the client can as it were download the result of the handling. Typically exceptionally advantageous in terms of time and speed in handling; Subsequently, the common result is that the GEE framework can process a huge sum of time series information (here partisan pictures) of distinctive regions of the world at a really tall speed and in a really brief time and display the comes about within the shape of different maps and charts.

REFERENCES

Arnold Jr, C. L., & Gibbons, C. J. 1996. Impervious Surface Coverage: The Emergence of a Key Environmental Indicator. *Journal of the American Planning Association*, 62(2), 243-258.

Attarchi, S. 2019. Efficiency Evaluation of SAR-Derived Indices in Urban Impervious Surfaces Extraction Using Full Polarimetric Image. *Geographical Urban Planning Research*, 7(4), 837-854. (In Persian)

Chunyang He, Peijun Shi, Dingyong Xie & Yuanyuan Zhao 2010. Improving the normalized difference build-up index to map urban built-up areas using a semiautomatic segmentation approach, *Remote Sensing Letters*, 1:4, 213-221, DOI: 10.1080/01431161.2010.481681

Esfandeh, S.; Danehkar, A.; Salmanmahiny, A.; Sadeghi, S.M.M.; Marcu, M.V. 2021. Climate Change Risk of Urban Growth and Land Use/Land Cover Conversion: An In-Depth Review of the Recent Research in Iran. Sustainability 2021, 14, 338.

Gates, David M. 1980: *Biophysical Ecology*, Springer-Verlag, New York, 611 p.

Goldblatt, R., You, W., Hanson, G., & Khandelwal, A. K. 2016. Detecting the Boundaries of Urban Areas in India: A Dataset for Pixel-Based Image Classification in Google Earth Engine. *Remote Sensing*, 8(8), 634.

Gomez-Chova, L., Fernández-Prieto, D., Calpe, J., Soria, E., Vila, J., & Camps-Valls, G. 2006. Urban Monitoring Using Multi-Temporal SAR and Multi-Spectral Data. *Pattern Recognition Letters*, 27(4), 234-243.

Haas, J., & Ban, Y. 2017. Sentinel-1A SAR and Sentinel-2A MSI Data Fusion for Urban Ecosystem Service Mapping. Remote Sensing Applications*: Society and Environment*, 8, 41–53.

Mohammadnejad, V. 2020. Urban lands Extraction from Sentinel 1 and 2 satellite imagery based on Google Earth Engine (GEE). *Geographical Urban Planning Research (GUPR)*, 8(3), 613-630. doi: 10.22059/jurbangeo.2020.301237.1270

Nasiri, V.; Deljouei, A.;Moradi, F.; Sadeghi, S.M.M.; Borz, S.A. 2022. Land Use and Land Cover Mapping Using entinel-2, Landsat-8 Satellite Images, and Google Earth Engine: A Comparison of Two Composition Methods. *Remote Sens.* 2022, 14, 1977. https://doi.org/10.3390/rs14091977

Patel, N. N., Angiuli, E., Gamba, P., Gaughan, A., Lisini, G., Stevens, F. R., & Trianni, G. 2015. Multitemporal Settlement and Population Mapping from Landsat Using Google Earth Engine. *International Journal of Applied Earth Observation and Geoinformation*, 35, 199–208.

Pavanelli, J. A. P., Santos, J. R. D., Galvão, L. S., Xaud, M., & Xaud, H. A. M. 2018. PALSAR- 2/ALOS-2 and OLI/LANDSAT-8 Data Integration for Land Use and Land Cover Mapping in Northern Brazilian Amazon. *Boletim De Ciências Geodésicas*, 24(2), 250–269.

Praticò, S.; Solano, F.; Di Fazio, S.; Modica, G. 2021. Machine Learning Classification of Mediterranean Forest Habitats in Google Earth Engine Based on Seasonal Sentinel-2 Time-Series and Input Image Composition Optimisation. *Remote Sens*. 2021, 13, 586.

Qian, X.; Zhang, L. 2022. An Integration Method to Improve the Quality of Global Land Cover. Adv. *Space Res*. 69, 1427–1438.

Rasoulinia M, Sharifi A. 2021. Potato yield estimation using Sentinel-2 satellite images, Case study: Sarab city. JGST. 2021; 11 (1) :107-116 URL: http://jgst.issge.ir/article-1-1015-fa.html

Schulz, D.; Yin, H.; Tischbein, B.; Verleysdonk, S.; Adamou, R.; Kumar, N. 2021. Land Use Mapping Using Sentinel-1 and Sentinel-2 Time Series in a Heterogeneous Landscape in Niger, Sahel. ISPRS J. Photogramm. *Remote Sens*. 2021, 178, 97–111.

Seto, K. C., Fragkias, M., Güneralp, B., & Reilly, M. K. 2011. A Meta-Analysis of Global Urban Land Expansion. Plos One, 6(8), E23777.

Shelestov, A., Lavreniuk, M., Kussul, N., Novikov, A., & Skakun, S. 2017. Exploring Google Earth Engine Platform for Big Data Processing: Classification of Multi-Temporal Satellite Imagery for Crop Mapping. *Frontiers in Earth Science*, 5, 17.

Shrestha, B., Ahmad, S. & Stephen, H. 2021. Fusion of Sentinel-1 and Sentinel-2 data in mapping the impervious surfaces at city scale. *Environ Monit Assess* 193, 556 2021. https://doi.org/10.1007/s10661-021-09321-6

Sobhani, P.; Esmaeilzadeh, H.; Barghjelveh, S.; Sadeghi, S.M.M.; Marcu, M.V. 2021. Habitat Integrity in Protected Areas Threatened by LULC Changes and Fragmentation: A Case Study in Tehran Province, *Iran. Land 2021*, 11, 6.

Viana, C.M.; Girão, I.; Rocha, J. 2019. Long-Term Satellite Image Time-series for land use/land cover change detection using refined open source data in a rural region. *Remote Sens*. 2019, 11, 1104.

Yao, Y.; Yan, X.; Luo, P.; Liang, Y.; Ren, S.; Hu, Y.; Han, J.; Guan, Q. 2022. Classifying Land-Use Patterns by Integrating Time-Series Electricity Data and High-Spatial Resolution *Remote Sensing Imagery*. Int. J. Appl. Earth Observ. Geoinf. 2022, 106, 102664.